Preprint typeset in JHEP style - HYPER VERSION DAMTP-2007-47

Particle transfer in braneworld collisions

Paul.M.Saffin[1]*and **Anders Tranberg**[2]†,

[1]*School of Physics and Astronomy, University of Nottingham*
University Park, Nottingham NG7 2RD, United Kingdom.
[2]*DAMTP, University of Cambridge*
Wilberforce Road, Cambridge, CB3 0WA, United Kingdom.

Abstract: We study the behaviour of fermions localized on moving kinks as these collide with either antikinks or spacetime boundaries. We numerically solve for the evolution of the scalar kinks and the bound (i.e. localized) fermion modes, and calculate the number of fermions transfered to the antikink and boundary in terms of Bogoliubov coefficients. Interpreting the boundaries as the brane on which we live, this models the ability of fermions on branes incoming from the bulk to "stick" on the world brane, even when the incoming branes bounce back into the bulk.

Keywords: Kinks, fermions, branes.

*email: paul.saffin@nottingham.ac.uk
†email: a.tranberg@damtp.cam.ac.uk

Contents

1. Introduction **1**

2. Scalar-fermion model in 1+1 dimensions **2**
2.1 Kinks and boundaries 4

3. Bound states **5**
3.1 Static kinks 5
3.2 Moving kinks 6
3.3 Boundaries 7

4. Kink dynamics **7**

5. Particle number and Bogoliubov coefficients **8**
5.1 Kink-antikink modes 8
5.2 Kink-boundary modes 11

6. Kink-antikink collisions **11**

7. Kink-boundary collision **13**

8. Conclusion **15**

1. Introduction

Fermions coupled to inhomogeneous background bosonic fields can become localised, in the sense that the fermion spectrum contains localised bound states [1, 2, 3]. In particular in the presence of scalar kinks, fermions prefer "living on" the kinks rather than populate higher energy (delocalised) radiation modes. This phenomenon is ubiquitous in condensed matter systems with impurities and where external magnetic (gauge) fields provide the inhomogeneities. The case of scalar fields acquires particular interest, if one allows kinks to represent higher dimensional domain walls or branes in string theory [4]. The localisation of fermions on inhomogeneities then becomes reminiscent of brane world scenarios, where the Standard Model fields are expected to "live" on one particular three dimensional brane.

In the presence of extra dimensions, additional branes may exist (in the "bulk"), each with their localised fermion states. As such branes collide, one may envisage fermions being transfered from one brane to another. Such a scenario was studied in [6].

Another picture of braneworlds emerges from the work of Horava and Witten [5], where it was realized that spacetime boundaries can play an important role. In that particular

case it was discovered that each of the two boundaries supported an E8 gauge theory. This braneworld model then places our Universe at the boundary of some larger spacetime. The question of what happens as bulk branes collide with our boundary-Universe is what this paper addresses, as well as extending the calculation of Gibbons *et al* [6].

In order to model a 3+1 Universe as a boundary of a 4+1 spacetime we could start with an action of Dirac fermions, and scalar fields that support domain walls to model the branes. However, if we employ a planar symmetry along the walls this model reduces to a 1+1 model with a boundary. And for our particular initial conditions (domain walls with just a bound zero mode) the equations for the Dirac fermion reduce to the equations for a Majorana fermion. So, while we in practise simulate a Majorana fermion in 1+1, this can be lifted to a 4+1 spacetime with Dirac fermions, a scalar field for the branes, and a boundary.

We study the fermion transfer numerically, treating the scalar as classical and the fermions in terms of a set of quantum modes.

2. Scalar-fermion model in 1+1 dimensions

We consider a model of a real scalar ϕ and a single fermion species ψ in 1+1 dimensional space-time. In our simulations we shall be considering situations both with and without a boundary, in either case the bulk action we use is

$$S_{\text{bulk}} = -\int dt\, dz \left[\frac{1}{2}\partial_\mu\phi\partial^\mu\phi - i\bar{\psi}\gamma^\mu\partial_\mu\psi + \frac{\lambda}{4}\left(\phi^2-1\right)^2 - ig\phi\bar{\psi}\psi\right], \tag{2.1}$$

with the bosonic boundary action being

$$S_{\text{boundary}} = \mp\int dt \left[\sqrt{\frac{\lambda}{2}}\left(\frac{1}{3}\phi^3-\phi\right)\right]_{z=0}, \tag{2.2}$$

Our choice of conventions is

$$\eta^{\mu\nu} = diag(-1,1), \quad \{\gamma_\mu,\gamma_\nu\} = 2\eta_{\mu\nu}, \quad \bar{\psi} = \psi^\dagger\gamma_0. \tag{2.3}$$

At this point, the couplings λ and g are free and we have chosen the boundary to lie at $z = 0$. The boundary action for the scalar may seem unnatural at first but, as we shall see, such a term means that there is no force between the boundary and a (static) kink, (or antikink if the + sign is chosen). Another reason is that this bosonic boundary term is required for the action to be supersymmetric, along with taking the spinor to be Majorana with couplings related by $g^2 = 2\lambda$. We shall not be requiring supersymmetry. The corresponding equations of motion in the bulk are

$$\left(\gamma^\mu\partial_\mu + g\phi(z,t)\right)\psi(z,t) = 0, \tag{2.4}$$

$$\left[\partial_\mu\partial^\mu - \lambda\left(\phi^2(z,t)-1\right)\right]\phi(z,t) = -ig\bar{\psi}\psi(z,t), \tag{2.5}$$

By choosing a real representation of γ_μ,

$$\gamma_0 = \begin{pmatrix} 0 & 1 \\ -1 & 0 \end{pmatrix}, \quad \gamma_z = \begin{pmatrix} 0 & 1 \\ 1 & 0 \end{pmatrix}. \tag{2.6}$$

the equation of motion for the complex two-component fermion splits up into two uncoupled real (Majorana) copies,

$$\psi = \psi_1^M + i\psi_2^M. \tag{2.7}$$

The equations of motion for ψ_1^M and ψ_2^M are identical, and we will from now on think in terms of a single, two-component Majorana fermion ψ_1^M, ignore the superscript, and write it as

$$\psi_1^M(z,t) = \begin{pmatrix} \psi_1(z,t) + \psi_2(z,t) \\ \psi_1(z,t) - \psi_2(z,t) \end{pmatrix}. \tag{2.8}$$

The equations of motion then read [1]

$$\dot{\psi_1}(z,t) = -\partial_z\psi_2(z,t) + g\phi\psi_2(z,t), \tag{2.9}$$
$$\dot{\psi_2}(z,t) = -\partial_z\psi_1(z,t) - g\phi\psi_1(z,t), \tag{2.10}$$
$$\ddot{\phi}(z,t) = \partial_z^2\phi(z,t) - \lambda\left(\phi^2(z,t) - 1\right)\phi(z,t) \tag{2.11}$$

We discretise these in a straightforward way and solve them numerically using a standard algorithm, 4th. order accurate in time, 2nd order in space. The boundary condition was satisfied using a Newton-Raphson iteration [16].

The boundary conditions coming from the action are

$$\partial_z\phi|_0 = \mp\sqrt{\frac{\lambda}{2}}\left(\phi^2 - 1\right)|_0, \tag{2.12}$$

and for the fermions we will be using

$$\psi_1|_0 = \mp\psi_1|_0,\ \psi_2|_0 = \pm\psi_2|_0, \tag{2.13}$$

which can be derived from a boundary action of $\pm\frac{i}{2}\int\ dt[\bar{\psi}\psi]_{z=0}$. We shall call these the $\mp$ Boundary Conditions, $\mp BC$. We see therefore that at the boundary either ψ_1 or ψ_2 vanishes, depending on the choice of sign of boundary conditions, with the $-BC$ giving $\psi_1|_0 = 0$ and the $+BC$ giving $\psi_2|_0 = 0$. As we shall see later, these boundary conditions allow for a normalizable fermion condensate on the boundary to co-exist with a kink or antikink.

The scalar field equation can be thought of as concerning a classical field, but as fermions are quantum, the right hand side source term should be replaced by $-ig\langle\bar{\psi}\psi\rangle$. The resulting equations amount to a quantum fermion in a classical scalar background.

For the purpose of this paper, we will make the approximation of neglecting the fermion back-reaction on the scalar. The upshot of this approximation is that whereas the solution of the mode equations (see below) are independent of the initial state (i.e. particle content) of those modes, the back-reaction term $\langle\bar{\psi}\psi\rangle$ is a quantum average over some density

[1] These equations are equivalent to those of the 4+1 system in [6] if we take $\psi_1 = i\psi_+$ and $\psi_2 = \psi_-$. This explains why the authors see an additional phase of $\pi/2$ between ψ_+ and ψ_-.

matrix. In the present context, we are more interested in the behaviour of the fermion modes as the scalar background changes than the exact details of the kink evolution. It is however clear that with many fermions present, in particular when including all the non-localised modes, the back-reaction may be sizeable, and may even drive the system to a high-temperature thermal state. Then the setup of a solitary kink or kink-antikink pair may no longer be realistic.

In our simulations we monitor the conservation of energy and we give here the expression of the energy in the scalar field,

$$H = \int dx \left[\frac{1}{2}(\dot{\phi})^2 + \frac{1}{2}(\phi')^2 + \frac{1}{2}\left(\frac{dW}{d\phi}\right)^2 \right] \pm W(z=0). \tag{2.14}$$

In particular we see that the boundaries have an energy associated with them. In the case where the scalar field is in the vacuum at the boundary we see that the boundary has an associated energy of

$$E_b(\phi=1) = \mp\frac{2}{3}\sqrt{\lambda/2}, \qquad E_b(\phi=-1) = \pm\frac{2}{3}\sqrt{\lambda/2}. \tag{2.15}$$

This boundary energy will be important in understanding the dynamics of kink-boundary collisions.

2.1 Kinks and boundaries

The static scalar equation of motion has a kink and an antikink solution ϕ_K and ϕ_A,

$$\phi_K(z) = \tanh\left(\frac{z-z_0}{D}\right), \quad \phi_A(z) = -\tanh\left(\frac{z-z_0}{D}\right), \quad D = \sqrt{\frac{2}{\lambda}}, \tag{2.16}$$

where z_0 is the center of the (anti-)kink. We will use $\lambda = 2$, $D = 1$ throughout.[2] Note that these static solutions obey

$$\partial_z \phi = \mp\sqrt{\frac{\lambda}{2}}\left(\phi^2 - 1\right), \tag{2.17}$$

so that there is no force between a kink and a $-BC$. Similarly there is no force between an antikink and the $+BC$. In the case where the coupling constants take the supersymmetric values, $g^2 = 2\lambda$, the (anti)kink and the $(+BC)-BC$ break the same half of the supersymmetry.

When colliding kink with antikink we shall employ periodic boundary conditions. When colliding single kinks onto a boundary, these are placed at $z = 0$, with the kink coming in from the left ($z < 0$). Note that there is no loss of generality by choosing to send in kinks but not antikinks, while using both boundary conditions. The system of kink and $-BC$ is equivalent to antikink and $+BC$, while kink and $+BC$ is equivalent to antikink and $-BC$; this covers all the possibilities.

[2]This amounts to rescaling the original action (2.1).

3. Bound states

3.1 Static kinks

An interesting facet of topological defects such as kinks is that they often allow for bound states in the particle spectrum. In the case at hand there are bound states for both the scalar and fermi fields. Indeed, the existence of the scalar bound state was the motivation behind the work of Rubakov and Shaposhnikov [13], asking whether we live on a domain wall. To study the scalar spectrum we consider perturbing the scalar equation of motion in (2.5) around a kink

$$\phi(z,t) = \phi_{\rm kink}(z) + \delta\phi(z,t), \tag{3.1}$$

then by writing

$$\delta\phi = \exp(i\omega t)F(z), \tag{3.2}$$

we solve the resulting eigenvalue equation to find the frequencies of the bound states [14, 13]. Taking the change of variables [6]

$$Z = \tanh(z/D), \tag{3.3}$$

we arrive at an associated Legendre equation with $l = 2$,

$$(1-Z^2)\frac{d^2F}{dZ^2} - 2Z\frac{dF}{dZ} + 2(2+1)F - \frac{(4-\omega^2D^2)}{1-Z^2}F = 0, \tag{3.4}$$

for which there are three solutions, $P_2^2(Z)$, $P_2^1(Z)$, $P_2^0(Z)$, corresponding to $m^2 = 4 - \omega^2D^2 = 2,\ 1,\ 0$. These give frequencies $\omega = 0,\ \sqrt{3}/D,\ 2/D$. The first of these modes, the zero mode, corresponds to the translation of the kink, the second is a true bound state while the third is not normalizable and so is not considered to be in the physical spectrum. We also note that this last solution is right on the boundary of the continuum states, which have mass $\sqrt{2\lambda} = 2/D$.

As well as these scalar bound states there are fermion modes localized to the kink which we now describe. First there is the zero-mode [1]

$$\psi_1^K(z,0) = \sqrt{\frac{\Gamma[gD+1/2]}{2D\sqrt{\pi}\Gamma[gD]}}\frac{1}{\cosh[(z-z_0)/D]^{gD}}, \quad \psi_2^K(z,0) = 0, \tag{3.5}$$

where we have normalized too unity according to the inner product

$$(\psi,\chi) = \int dx \psi^\dagger \chi. \tag{3.6}$$

Now recall that the scalar field of the kink can happily co-exist with the -BC, and that these boundary conditions required the vanishing of $\psi_2(z=0)$. So we see that the -BC also have no effect on the fermion fields of the static kink.

In addition to the zero mode we also find that there is an excited fermion mode given by

$$\psi_1^{KE}(z,t) = -\mathcal{N}\omega D \frac{\sinh\left(\frac{z-z_0}{D}\right)}{\left[\cosh\left(\frac{z-z_0}{D}\right)\right]^{gD}} \cos(\omega t - \varphi), \tag{3.7}$$

$$\psi_2^{KE}(z,t) = \mathcal{N} \frac{1}{\left[\cosh\left(\frac{z-z_0}{D}\right)\right]^{gD-1}} \sin(\omega t - \varphi), \tag{3.8}$$

with

$$\omega^2 = \frac{2gD-1}{D^2}, \quad \mathcal{N}^2 = \frac{(gD-1)\,\Gamma[gD+1/2]}{(2gD-1)\,D\sqrt{\pi}\Gamma[gD]}. \tag{3.9}$$

Recall that this model, with a Majorana fermion, is supersymmetric when $g = \sqrt{2\lambda} = 2/D$. In this case we see that the frequency of the excited fermion mode matches that of the scalar bound state, $\omega = \sqrt{3}/D$, as is expected for supersymmetry. We also expect, given that there are no more scalar bound states, that there will be no more fermion excited states. We note that this does not hold true as we change couplings away from the supersymmetric case.[3]

3.2 Moving kinks

As we are interested in kinks colliding with each other and against boundaries we need to know what kinks and bound states look like when they are moving, that is, we need to boost the kink.

The scalar field of a kink (antikink) moving at speed v simply involves a Lorenz contraction by $\gamma = 1/\sqrt{1-v^2}$,

$$\phi_v^{K/A}(z,0) = \pm \tanh\left[\gamma\left(\frac{z-z_0}{D}\right)\right]. \tag{3.10}$$

An isolated, moving kink or antikink has an energy of

$$E_{\text{antikink}} = E_{\text{kink}} = \frac{4}{3}\sqrt{\lambda/2}\gamma. \tag{3.11}$$

We note that the energy of a static kink, $v = 0$ coincides with the difference in energy between a $-$ and a $+$ boundary, $\Delta E_{\text{b}} = \frac{4}{3}\sqrt{\lambda/2}$, from Eq. (2.15).

The fermion modes also transform in the usual way, and in terms of the $1, 2$ components we have

$$\psi_1(z,t) \to \psi'_{1,v}(z,t) = \sqrt{\frac{\gamma+1}{2}}\left(\psi_1\left[\gamma(z-vt)\right] + \frac{v\gamma}{\gamma+1}\psi_2\left[\gamma(z-vt)\right]\right), \tag{3.12}$$

$$\psi_2(z,t) \to \psi'_{2,v}(z,t) = \sqrt{\frac{\gamma+1}{2}}\left(\psi_2\left[\gamma(z-vt)\right] + \frac{v\gamma}{\gamma+1}\psi_1\left[\gamma(z-vt)\right]\right). \tag{3.13}$$

[3]We would like to thank Kei-ichi Maeda for informing us of his calculation showing that there is a tower of bound states with frequency $\omega^2 = n\frac{2gD-n}{D^2}$, for integer n subject to $0 \le n < gD$.

3.3 Boundaries

Just as kinks support bound states, so does a boundary. To describe these we consider the scalar field to be in one of its vacuum states at the boundary, $\phi(z=0)=\pm 1$, then we see from the spinor equations of (2.9) that the boundary carries a single localized, normalisable fermion

$$\partial_z \psi_1(z) = -g\phi(z)\psi_1(z), \quad \partial_z \psi_2(z) = g\phi(z)\psi_2(z). \tag{3.14}$$

For $\phi(z=0)=+1$ the normalisable solution is given by

$$\psi_1^B(z) = 0, \quad \psi_2^B(z) = \sqrt{g}\exp(gz). \tag{3.15}$$

For $\phi(z=0)=-1$ we instead have

$$\psi_1^B(z) = \sqrt{g}\exp(gz), \quad \psi_2^B(z) = 0. \tag{3.16}$$

Note that the condition of normalisability imposes that one fermion component is zero in each case. For example, if we have a single kink in the bulk (which allows a condensate of ψ_1) then at the boundary we will have $\phi \simeq +1$ which allows a boundary condensate of ψ_2, consistent with the -BC.

4. Kink dynamics

Before discussing the behaviour of fermions on kinks we first want to describe how kinks interact with antikinks, and also how they interact with the $\pm BC$ boundaries. The dynamics of kink-antikink collisions have been studied by a number of authors [7, 8, 9, 10, 11] revealing the rich structure of behaviour at small impact speeds, v. At large speeds, $v \gtrsim 0.2$, the kinks simply collide a single time and bounce away to infinity. As we go to smaller speeds then the kinks may have multiple collisions before travelling off to infinity, or they may simply annihilate. While extending the analysis of [6] for the fermions involved in such collisions we shall concentrate on the simplest range of speeds where there is a single collision, Fig. 1.

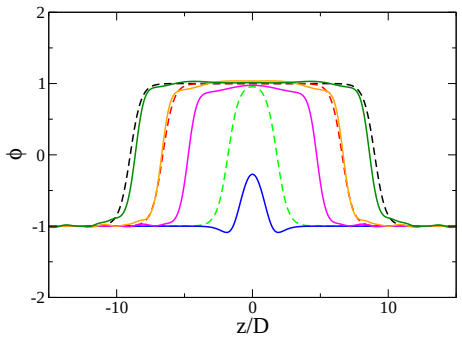

Figure 1: The incoming kink profiles before, during and after a kink-antikink collision. The curves are equally spaced in time, with dashed lines before the collision and full lines after.

In order to capture the dynamics of brane-boundary collisions, Antunes *et al* [16] modelled the system with a scalar field and, in our language, collided kinks against $\pm BC$-like boundaries. They discovered that the kink is temporarily absorbed into the boundary, but re-emerges having lost a (model-independent) fraction of its kinetic energy of $\sim 63\%$.

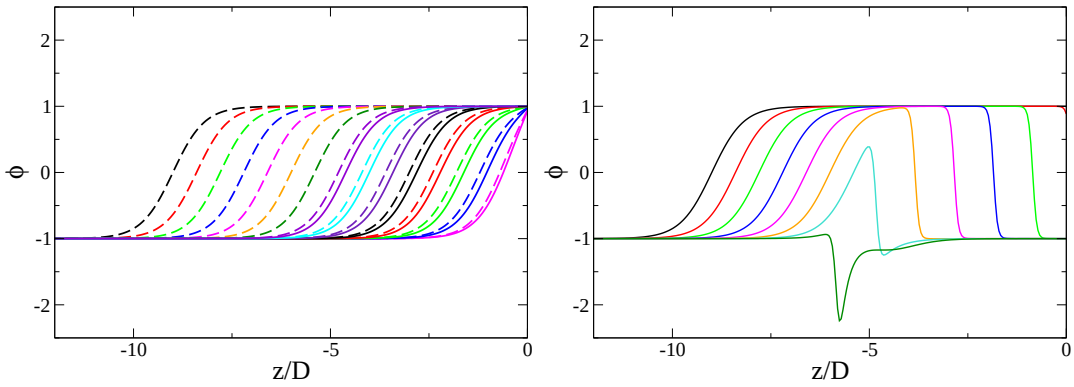

Figure 2: The incoming kink profiles before and after the collision with a $-BC$ boundary (left). The curves are equally spaced in time, dashed before the collision, full after. The kink enters the boundary and comes back out unscathed. In contrast, the $+BC$ boundary (right) decays straight away and emits an antikink which prevents the incoming kink from reaching the boundary.

The boundary conditions used were in fact slightly different from ours, in that they made the replacement

$$W'(\phi) = \pm\sqrt{\frac{\lambda}{2}}(\phi^2 - 1) \;\rightarrow\; |\sqrt{\frac{\lambda}{2}}(\phi^2 - 1)|, \tag{4.1}$$

hence having $-BC$ between the two potential minima and $+BC$ outside. This fix is responsible for the reported energy loss at collision.

In our simulations we shall be re-visiting this scenario, but using strict $\pm BC$ boundaries. Then energy is conserved at collision, taking into account changes in boundary energy. For $-BC$, the kink reemerging from the boundary has equal and opposite velocity to the incoming one, Fig. 2 (left). In the case of $+BC$ the vev $\phi(z=0) = 1$ at the boundary is unstable to decay via the emission of an antikink, Fig. 2 (right). This because the energy difference between $+1$ and -1 on the boundary is exactly the energy of an antikink. In the absence of an incoming kink (or with a kink very far away), the boundary could remain in the unstable vacuum, but as the kink approaches, the exponential tail hits the wall and causes the vacuum to decay. In practice, this means that before the kink reaches the boundary, an antikink will be emitted and collide with the incoming kink. Hence we cannot realise a kink/$+BC$ collision.

5. Particle number and Bogoliubov coefficients

5.1 Kink-antikink modes

The general philosophy to calculating particle numbers is to identify the correct vacuum and creation/annihilation operators. For example, when colliding a kink and antikink we consider the system in the asymptotic past to be in a vacuum state and we can therefore expand the fermi wave operator as

$$\Psi = a^K \psi_{in}^K + a^{KE} \psi_{in}^{KE} + a^A \psi_{in}^A + a^{AE} \psi_{in}^{AE} + \text{continuum}. \tag{5.1}$$

Where the a are the particle operators for: the fermi zero mode on the kink (K); fermi zero mode on the antikink (A); first excited fermi mode on the kink (KE); first excited fermi mode on the antikink (AE). And the ψ_{in} are the (normalized) mode functions found in section 3 corresponding to kinks and antikinks with the requisite position and velocity. If there is more than one excited fermion mode then they may also be included in an obvious way. To an observer in the asymptotic future there will be a similar expansion, only now they will use a different set of particle operators,

$$\Psi = b^K \psi^K_{out} + b^{KE} \psi^{KE}_{out} + b^A \psi^A_{out} + b^{AE} \psi^{AE}_{out} + \text{continuum}. \tag{5.2}$$

Again, the mode functions ψ_{out} are the mode functions corresponding to the kink, antikink with the appropriate position and velocity of the outgoing defects.

From the original action we see that the momentum conjugate to the wave operator Ψ is $i\Psi^\dagger$ so by using the standard equal-time anti-commutation relation

$$\{\Psi_\alpha(t, \underline{x}), \Psi^\dagger_\beta(t, \underline{y})\} = \delta_{\alpha,\beta}\delta(\underline{x} - \underline{y}), \tag{5.3}$$

we see that the particle operators obey

$$\{a, a^\dagger\} = \{b, b^\dagger\} = 1, \tag{5.4}$$

with other anti-commutators vanishing.

Now that we have our wave operator in the asymptotic limits, we need to relate the particle operators in order to understand how particle numbers are affected. To do this we introduce the Bogoliubov coefficients in the standard way, which relate the mode functions ψ_{in} to ψ_{out} in the asymptotic future. In the following expressions the mode functions ψ_{in} are the time-evolved mode functions from (5.1) evaluated in the asymptotic future,

$$\begin{aligned}
\psi^K_{in} &= \alpha_K \psi^K_{out} + \beta_K \psi^{KE}_{out} + \gamma_K \psi^A_{out} + \delta_K \psi^{AE}_{out} \ + \ \text{continuum}, \\
\psi^{KE}_{in} &= \alpha_{KE} \psi^K_{out} + \beta_{KE} \psi^{KE}_{out} + \gamma_{KE} \psi^A_{out} + \delta_{KE} \psi^{AE}_{out} \ + \ \text{continuum}, \\
\psi^A_{in} &= \alpha_A \psi^K_{out} + \beta_A \psi^{KE}_{out} + \gamma_A \psi^A_{out} + \delta_A \psi^{AE}_{out} \ + \ \text{continuum}, \\
\psi^{AE}_{in} &= \alpha_{AE} \psi^K_{out} + \beta_{AE} \psi^{KE}_{out} + \gamma_{AE} \psi^A_{out} + \delta_{AE} \psi^{AE}_{out} \ + \ \text{continuum},
\end{aligned} \tag{5.5}$$

The α_i, β_i, γ_i, δ_i are the Bogoliubov coefficients, which can be extracted by taking the inner products according to (3.6)

$$\alpha_K = (\psi^K_{in}, \psi^K_{out}), \qquad \beta_K = (\psi^K_{in}, \psi^{KE}_{out}), \tag{5.6}$$

$$\gamma_K = (\psi^K_{in}, \psi^A_{out}), \qquad \delta_K = (\psi^K_{in}, \psi^{AE}_{out}), \tag{5.7}$$

and similarly for ψ_{KE}, ψ_A, ψ_{AE}, ψ_B. In this way we are able to calculate all of the Bogoliubov coefficients for a given simulation.

The number operator takes the standard form,

$$\hat{N} = \frac{1}{2} \int dx (\Psi^\dagger \Psi - \Psi \Psi^\dagger), \tag{5.8}$$

which we may write, using (5.1), (5.2), (5.4), in terms of the particle operators

$$\hat{N} = \hat{n}^K + \hat{n}^{KE} + \hat{n}^A + \hat{n}^{AE}, \tag{5.9}$$

$$\hat{n}^K = \mathcal{O}^{K\dagger}\mathcal{O}^K - \frac{1}{2}, \quad \hat{n}^A = \mathcal{O}^{A\dagger}\mathcal{O}^A - \frac{1}{2}, \tag{5.10}$$

$$\hat{n}^{KE} = \mathcal{O}^{KE\dagger}\mathcal{O}^{KE} - \frac{1}{2}, \quad \hat{n}^{AE} = \mathcal{O}^{AE\dagger}\mathcal{O}^{AE} - \frac{1}{2}, \tag{5.11}$$

where $\mathcal{O}$ represents either the a or b particle operator depending on whether we are looking at the past or future respectively. We define the vacuum relative to the initial state as

$$\forall\ i, j, \quad a^i|0\rangle = 0, \tag{5.12}$$

and the particle states as

$$|K000\rangle = a^{K\dagger}|0\rangle, \quad |0A00\rangle = a^{A\dagger}|0\rangle, \quad |00KE0\rangle = a^{KE\dagger}|0\rangle, \quad |000AE\rangle = a^{AE\dagger}|0\rangle. \tag{5.13}$$

We can see from this that, as described in [1], the vacuum states have fermion number $-\frac{1}{2}$ whilst the excited states have fermion number $+\frac{1}{2}$.

We are now in a position to express the asymptotic-future particle operators, b, in terms of the asymptotic past particle operators, a, by comparing (5.1) and (5.2) and using (5.5),

$$b^K = \alpha_K a^K + \alpha_{KE} a^{KE} + \alpha_A a^A + \alpha_{AE} a^{AE}, \tag{5.14}$$

$$b^{KE} = \beta_K a^K + \beta_{KE} a^{KE} + \beta_A a^A + \beta_{AE} a^{AE}, \tag{5.15}$$

$$b^A = \gamma_K a^K + \gamma_{KE} a^{KE} + \gamma_A a^A + \gamma_{AE} a^{AE}, \tag{5.16}$$

$$b^{AE} = \delta_K a^K + \delta_{KE} a^{KE} + \delta_A a^A + \delta_{AE} a^{AE}. \tag{5.17}$$

For simplicity, we will focus our interest on evaluating the expectation values in the state corresponding to a kink with a zero mode fermion colliding with a vacuum antikink.

$$n^K = \langle K000|b^{K\dagger}b^K|K000\rangle - 1/2, \tag{5.18}$$

and similarly for n^{KE}, n^A, n^{AE}, n^B. These then represent the fermion occupation numbers in the respective modes after the collisions, assuming that the initial state has only excitations (particles) in the kink fermion groundstate. This state is annihilated by all the $a^{KE/A/AE}$, leaving us to calculate only

$$n^K + 1/2 = \left(n_0^K + 1/2\right)|\alpha^K|^2, \tag{5.19}$$

$$n^{KE} + 1/2 = \left(n_0^K + 1/2\right)|\beta^K|^2, \tag{5.20}$$

$$n^A + 1/2 = \left(n_0^K + 1/2\right)|\gamma^K|^2, \tag{5.21}$$

$$n^{AE} + 1/2 = \left(n_0^K + 1/2\right)|\delta^K|^2, \tag{5.22}$$

where we have generalised to an initial state with fermions only in the K mode, but with an arbitrary particle number n_0^K. We will not be concerned with the normalisation of the state, but simply compute the Bogoliubov coefficients α_K, β_K, γ_K, δ_K. Below we will suppress the label K.

5.2 Kink-boundary modes

For the collision of a kink on a $-BC$, we now expand the wave operator as

$$\Psi = a^K \psi^K_{in} + a^{KE} \psi^{KE}_{in} + a^B \psi^B_{in} + \text{continuum}. \tag{5.23}$$

and

$$\Psi = b^K \psi^K_{out} + b^{KE} \psi^{KE}_{out} + b^B \psi^B_{out} + \text{continuum}, \tag{5.24}$$

where the index B refers to the boundary zero mode. The expansion of the mode functions proceeds as before, with the addition of a boundary mode function,

$$\psi^K_{in} = \alpha_K \psi^K_{out} + \beta_K \psi^{KE}_{out} + \xi_K \psi^B_{out} \ + \ \text{continuum}, \tag{5.25}$$

$$\psi^B_{in} = \alpha_B \psi^K_{out} + \beta_B \psi^{KE}_{out} + \xi_B \psi^B_{out} \ + \ \text{continuum}, \tag{5.26}$$

and if we send in a kink with non-vanishing occupation number n^0_K for the zero-mode fermion, then we find that the boundary number operator in the asymptotic future is

$$n^B + 1/2 = \left(n^K_0 + 1/2\right) |\xi^K|^2. \tag{5.27}$$

6. Kink-antikink collisions

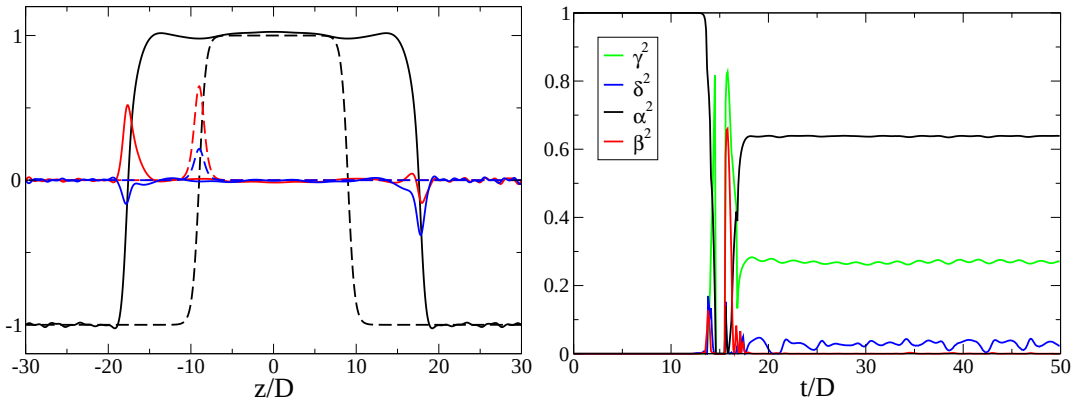

Figure 3: Left: The scalar field (black) and the fermion K mode components ψ_1 (red) and ψ_2 (blue) before (dashed) and after (full) the collision. The initial velocity was $v = 0.6$, and the coupling $g = 2$. Right: The overlap of the incoming K mode after the collision with the outgoing kink K and antikink A modes (α and γ), and the KE and AK modes (β and δ).

The first set of results that we shall present is an extension of the study in [6], where the Bogoliubov coefficients of the fermion zero mode were calculated for kink/antikink collisions. Here we also present data for the excited fermion bound state, as well as observing the dependence on collision speed.

The collisions were performed by initially placing a kink and a antikink a distance $30v$ apart. We then boosted them with velocity v and $-v$ respectively, as described above. Fig. 3 (left) shows the profile of the scalar field and fermion modes before and after the

collision, for the case of $v = 0.6$, $g = 2$. Both before and after the collision, the fermion modes are well localised around the kink and antikink.

We then calculate the Bogoliubov coefficients in time, Fig. 3 (right). Before the collision at $Dt \simeq 15$ the fermion mode is the kink K mode, and so $|\alpha|^2 = 1$. during the collision all bets are off; in particular we are not able to assign velocities to individual kinks. Already at time $Dt = 20$, the kink-antikink pair have disentangled themselves, and a final Bogoliubov coefficient had been established. Although there is some residual oscillation even at late times, we assign final values at $Dt = 50$.

It is worth noting, that because the phase φ in Eqs. (3.7, 3.8) is undetermined, we instead keep the whole time-dependence $\omega t + \varphi$ fixed when computing the overlap. This means that the computed β and δ are oscillating functions in time, Fig. 3 (right), and we should use the amplitude of this oscillation as the Bogoliubov coefficient. Taking this

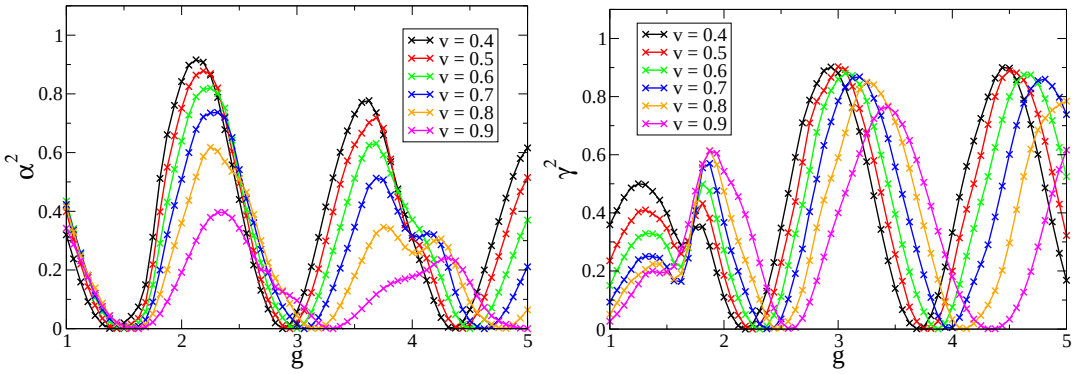

Figure 4: Left: The velocity and coupling dependence of the Bogoliubov coefficients of the incoming K mode with the outgoing K mode. Right: The same for the overlap on the A mode. Errorbars reflecting the residual oscillation (see text) are roughly the size of the symbols.

into account, the Bogoliubov coefficients can be read off with an accuracy of in most cases better than 0.01. Fig. 4 shows the g and v dependence of α^2 and γ^2, the overlap with the outgoing K and A modes.

As noted in [6], the coupling dependence approximately follows a $a+b\sin(cg+d)$ form, although the amplitude decreases somewhat with g, especially for α. We will not attempt to fit this behaviour numerically, but simply note some qualitative points of interest. α^2 and γ^2 are anti-correlated with the same period in g, and the bulk of the fermion number ends up in these lowest energy modes after the collision. However, as v is increased, fermion number is lost from these modes, in particular from α^2. For small g, the Bogoliubov coefficients take a very long time to settle and seem to decrease continuously until they do so. Fig. 5 shows the corresponding overlap with the KE and AE modes, β^2 and δ^2. These are strongly correlated with each other and seem to have the same period in g as K/A mode coefficients, but with a phase shift of $\pi/2$. The fermion number taken away in these modes is much smaller, but it is interesting that up to 10 to 20 percent can end up here. There is a mild increase with v consistent with the decrease in α^2 and γ^2.

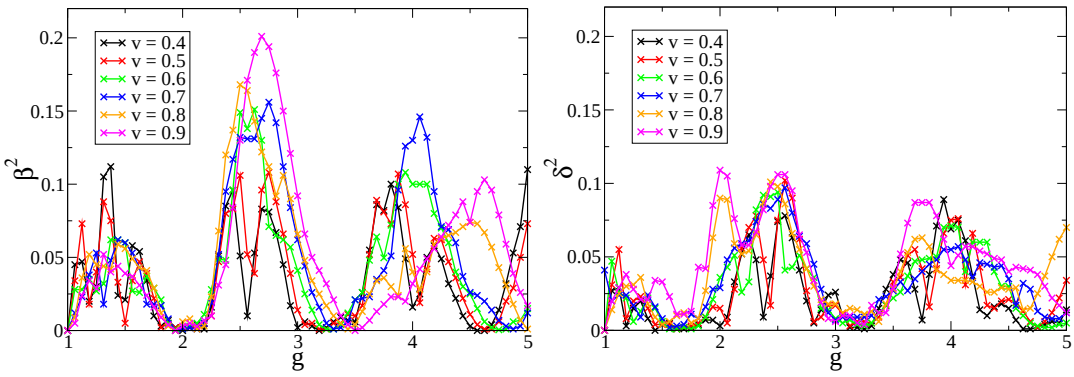

Figure 5: Left: The velocity and coupling dependence of the Bogoliubov coefficients of the K mode with the outgoing kink KE mode. Right: The same for the overlap on the antikink AE mode.

Any missing fermion number must then be transfered to modes which we do not take into account, radiation or additional time-dependent bound states. We quantify this by calculating the sum of the coefficients $|\alpha|^2 + |\beta|^2 + |\gamma|^2 + |\delta|^2$, shown in Fig. 6. The loss to radiation has some non-trivial dependence on g, and increases with v, presumable because there is then energy available to excite higher energy modes. It is striking that up to 60 percent of the fermion number can be lost to radiation in this way.

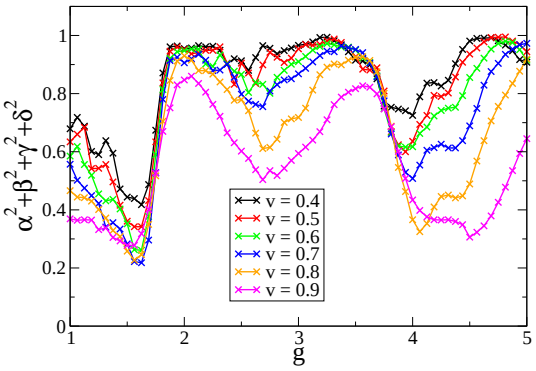

Figure 6: The sum of Bogoliubov overlaps on all the bound states $|\alpha|^2 + |\beta|^2 + |\gamma|^2 + |\delta|^2$. The deviation from 1 is the amount of fermion number carried away as radiation.

7. Kink-boundary collision

The second set of results in this paper are those associated with a brane colliding into a boundary, rather than another brane. as such, we now collide a single kink onto $-BC$ boundary and see to what extent a fermion originally localised on the kink will stick to the boundary. Fig. 7 (left) shows the field profiles initially and at late times after the collision. Again, the fermions remain nicely localised around the kink, but after the collision also at the boundary.

We shall again consider only the case where the kink starts with a fermion zero mode, and calculate the Bogoliubov coefficient for finding a fermion in the outgoing K ($|\alpha|^2$), the outgoing KE ($|\beta|^2$) and the boundary B ($|\xi|^2$) modes. Fig. 7 (right) show the coefficients in time, again with $\alpha^2 = 1$ until the collision at $Dt \simeq 15$. After another transient collision stage, the coefficients take on definite values, and we end the simulation at $Dt = 50$. The results concerning fermions radiating into the bulk are somewhat different to the kink/antikink collisions. As shown in Fig. 9 we see that the sum representing bound state fermions, $|\alpha|^2+|\beta|^2+|\xi|^2$, is very close to unity. This implies that very little of the fermions

end up in the bulk, with larger collision speeds producing more bulk fermions as one would expect. We again determine the dependence on g and v, shown in Fig. 8. In this case α^2 is

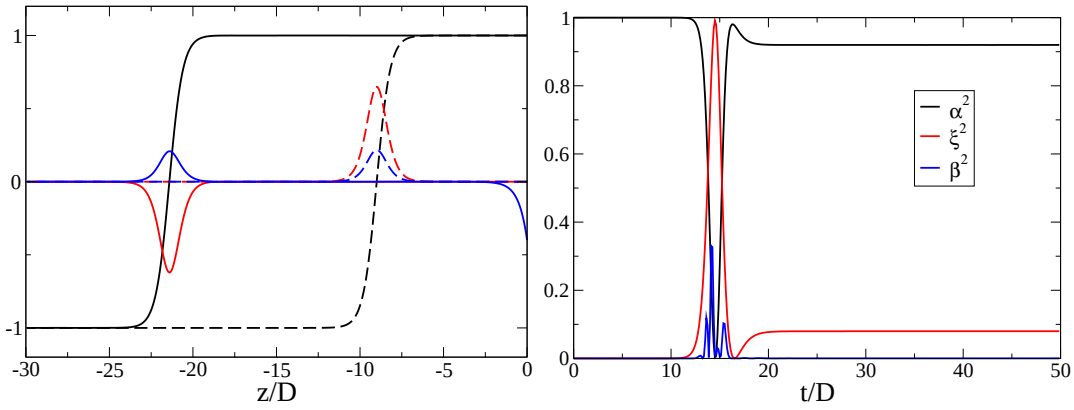

Figure 7: Left: The scalar field (black) and the fermion K mode components ψ_1 (red) and ψ_2 (blue) before (dashed) and after (full) the collision. The initial velocity was $v = 0.6$, and the coupling $g = 2$. Note the non-zero boundary mode contribution to the far right. Right: The overlap of the K mode after the collision with the outgoing kink K and KE modes (α and β) and the boundary mode B (ξ).

almost exactly anti-correlated with ξ^2. Most fermion number is transfered to the boundary for small and large values of g, with the maxima moving down and up , respectively as v is increased. For $v = 0.9$, the kink retains its fermion, at least in the range of couplings used here.

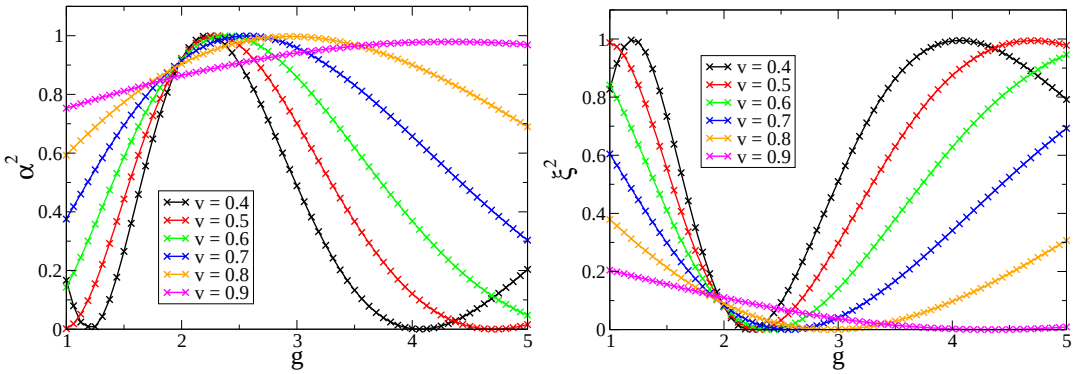

Figure 8: The Bogoliubov coefficients of the incoming K mode unto the outgoing K mode, $|\alpha|^2$, (left) and B mode, $|\xi|^2$, (right).

In order to understand the kink/antikink results we repeat the approximation developed in [6]. The approximation is a way of solving (2.5), (2.10) which writes the fermi field during the collisions as

$$\psi_{(1,2)} \simeq A_{(1,2)} f(z), \tag{7.1}$$

where $f(z)$ is some even, normalized function, and the total amplitude is normalized by

$A^2_{(1)} + A^2_{(2)} = 1$. We then find that (2.5), (2.10) may be integrated along the z axis to give

$$A^2_{(1,2)} \simeq \frac{1}{2}\left(1 + \sin(2g\phi_c \Delta t)\right). \tag{7.2}$$

In this expression we have a representative value for ϕ during the collision, ϕ_c, and a collision timescale Δt. In this way Gibbons *et al* were able to explain the sinusoidal behaviour of the Bogoliubov coefficients when a kink collides with an antikink. Unfortunately, the case of a kink colliding with a boundary does not succumb to the same analysis, largely because the fermion mode functions have rather different z-dependence owing to one of them being forced to vanish at the boundary. However, from the form of the Bogoliubov coefficients it is tempting to speculate that a relation similar to (7.2) holds. A possible explanation for the longer "wavelengths" in Fig. 8 could then be that during the kink/boundary collision the value of ϕ changes very little from its vacuum value, while in the kink/antikink collisions one finds that ϕ overshoots the vacuum by some amount depending on collision speed.

8. Conclusion

In summary, we have performed a detailed numerical study of fermion transfer in kink-antikink and kink-boundary collisions.

In kink-antikink collisions, we confirm the findings of Gibbons *et al* [6] that although the scalar field kinks bounce off each other in an elastic way, fermions initially in the K mode on the kink will be distributed on the K, A, and radiation modes. As an extension of their work we also included the first fermion excited modes, KE, AE, finding that these modes also gets excited, and presented data for a wide range of collision speeds. The distribution is very sensitive to the value of the coupling g, and hence the mass of the fermions $g\phi$. For small incident velocities v, most of the fermion number ends up in the K and A modes, and these are anti-correlated in g. As the velocity is increased, more and more fermion number is transfered from the K/A modes to the KE and AE, but also delocalised radiation modes, and up to 60 percent can be "lost" to the bulk.

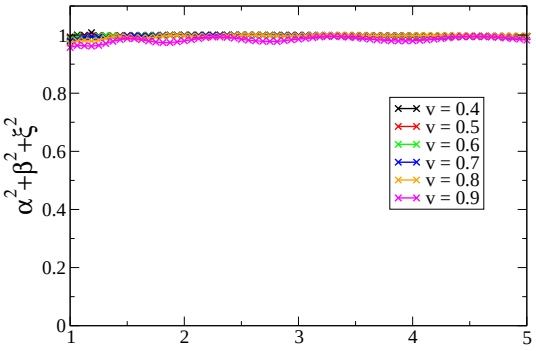

Figure 9: The sum, $|\alpha|^2 + |\beta|^2 + |\xi|^2$, representing the fraction of fermions that end up in bound states.

When colliding kinks on a -BC boundary, we found again that the kink is reflected elastically, but that a significant amount of fermion number can stick on the boundary. In this case, the K and B modes are anticorrelated in g, but in contrast to the kink-antikink collisions, very little fermion number is transfered to the KE mode or radiation. For the values of g employed here, low v favours transfer to the boundary, whereas for high v the fermions stay on the kink and are carried away from the boundary again.

We in fact also solved for the evolution of the initial B, A, KE, and AE modes, and unsurprisingly found that fermions initially in these modes are also distributed on all modes after collision. In particular, a fermion localised on the boundary can be carried away by

a kink bouncing on this boundary. For brevity and to focus on our main aim, we did not carry out a detailed exposition of all mode combinations. It is however straightforward to do so.

We found that the numerical implementation of the $\pm BC$ boundary conditions require some care, and that discretisation errors can be significant. We dealt with this by using iterative methods, higher order derivatives and rather fine lattices, $Ddr = 0.0025$.

One could consider including more and more fermion modes in the spectrum, in order to track the "lost" fermions. In the end, this would lead to a full quantum (Hartree) treatment [18], and one would be able to include the back-reaction on the scalar self-consistently. For the purpose of this paper, we found the K, A, KE, AK and B modes to be sufficient.

We started by arguing that our 1+1 model could be lifted to give results for a 4+1 spacetime. While this is true, one has ignored any effects that depend on the directions within the brane. In particular we have not presented any results about the $\underline{k}$ dependence of the Bogoliubov coefficients (where $\underline{k}$ refers to the wave-number in the brane world-volume.) We hope to present results on this in a future publication.

Another natural extension of this work is to consider more than one species of fermions and/or more scalars to include effects like C and CP violation in the scalar-fermion interaction. This would for instance be relevant to electroweak baryogenesis, where at a first order phase transition, a domain wall sweeps through a plasma, reflecting fermions off it in a CP-violating way.

Acknowledgments

We thank Kei-Ichi Maeda for stimulating discussions. P.M.S is supported by PPARC and A.T. is supported by PPARC Special Programme Grant *"Classical Lattice Field Theory"*. We gratefully acknowledge the use of the UK National Cosmology Supercomputer, Cosmos, funded by PPARC, HEFCE and Silicon Graphics.

References

[1] R. Jackiw and C. Rebbi, Phys. Rev. D **13**, 3398 (1976).

[2] R. Jackiw and P. Rossi, Nucl. Phys. B **190**, 681 (1981).

[3] A. J. Niemi and G. W. Semenoff, Phys. Rept. **135**, 99 (1986).

[4] O. DeWolfe, D. Z. Freedman, S. S. Gubser and A. Karch, Phys. Rev. D **62**, 046008 (2000) [arXiv:hep-th/9909134].

[5] P. Horava and E. Witten, Nucl. Phys. B **475**, 94 (1996) [arXiv:hep-th/9603142].

[6] G. Gibbons, K. i. Maeda and Y. i. Takamizu, Phys. Lett. B **647** (2007) 1 [arXiv:hep-th/0610286].

[7] P. Anninos, S. Oliveira and R. A. Matzner, Phys. Rev. D **44**, 1147 (1991).

[8] V. Silveira, Phys. Rev. D **38**, 3823 (1988).

[9] T. I. Belova and A. E. Kudryavtsev, "Quasiperiodical Orbits In The Scalar Classical Lambda Phi**4 Field Physica D **32**, 18 (1988).

[10] D. K. Campbell, J. F. Schonfeld and C. A. Wingate, Physica **9D**, 1 (1983).

[11] Y. i. Takamizu and K. i. Maeda, Phys. Rev. D **70**, 123514 (2004) [arXiv:hep-th/0406235].

[12] Y. i. Takamizu, H. Kudoh and K. i. Maeda, Phys. Rev. D **75** (2007) 061304 [arXiv:gr-qc/0702138].

[13] V. A. Rubakov and M. E. Shaposhnikov, Phys. Lett. B **125**, 136 (1983).

[14] R. F. Dashen, B. Hasslacher and A. Neveu, Phys. Rev. D **10**, 4130 (1974).

[15] Y. i. Takamizu and K. i. Maeda, Phys. Rev. D **73** (2006) 103508 [arXiv:hep-th/0603076].

[16] N. D. Antunes, E. J. Copeland, M. Hindmarsh and A. Lukas, Phys. Rev. D **69** (2004) 065016 [arXiv:hep-th/0310103].

[17] S. Randjbar-Daemi and M. E. Shaposhnikov, Phys. Lett. B **492** (2000) 361 [arXiv:hep-th/0008079].

[18] G. Aarts and J. Smit, Nucl. Phys. B **555** (1999) 355 [arXiv:hep-ph/9812413].